

## Seismic evaluation of Hybrid steel frames with different patterns of semi-rigid connection

M. Ghassemieh<sup>1)</sup> and N. Vahedi<sup>2)</sup>

<sup>1)</sup> School of Civil Engineering, University of Tehran, Tehran, Iran

<sup>2)</sup> MSc. Student of Structural Engineering, School of Civil Engineering, University of Tehran, Tehran, Iran, (+98)9127904126,

[mghassem@ut.ac.ir](mailto:mghassem@ut.ac.ir)

[nvahedi690@ut.ac.ir](mailto:nvahedi690@ut.ac.ir)

### ABSTRACT

Hybrid steel frame is a new lateral resistant steel moment frame which is a mixture of fully-rigid and semi-rigid steel connections. In this research, the seismic performance of several different patterns and locations of semi-rigid connections, within the 9-story SAC frame (mid-rise building) is examined. Static pushover analysis, cyclic displacement history and nonlinear dynamic analysis are conducted on the proposed selected frames. The performance of frames are evaluated based on maximum normalized base shear, energy dissipation and maximum story drift angle during seismic records. During the process of modeling, plastic hinges in beams and semi-rigid connections are considered as the main sources of nonlinearity and they are simulated by lumped plasticity models. The results indicate that the hybrid frame can improve and enhance the performance in comparison with rigid frame if the frame is correctly proportioned.

**Keywords:** Hybrid steel frame, seismic performance, semi-rigid, SAC frame.

### INTRODUCTION

The Northridge earthquake severely damaged many concrete and steel structures; while steel building performed seemingly well. However, a closer inspection discovered many beam-to-column connections in steel frames had failed in a brittle matter [1]. Numerous factors have been identified which were potentially contributed to the poor seismic performance of the Pre-Northridge steel moment connections. Failure happened due to different combination of those factors: workmanship and inspection quality, weld design, fracture mechanics, base metal elevated yield stress, weld stress condition, stress concentration, effect of triaxial stress condition, loading rate and presence of composite floor slab [1]. Two key strategies have been developed to overcome the problem. One method to improve the performance of existing building is to increase the beam capacity at the column face by supplying cover plates [1]. FEMA 355c suggests placing haunches or

---

<sup>1)</sup> Professor

<sup>2)</sup> MSc. Student

ribs as an alternative to the cover plates. As a result, the panel zone is stiff, and the beam is able to reach inelastic behavior before failure occurs [1]. Another method is to decrease the beam flanges at the locations where plastic hinges were initially assumed to develop [1]. This approach is termed the Reduced Beam Section (RBS) method, and it successfully shifts the seismic demand from the connection to the beam, where damage can be controlled [1].

The expected performance of steel moment frames in energy dissipation and flexibility under lateral loads was sacrificed after the 1994 Northridge earthquake when the steel moment frame did not perform as expected. This problem motivated researchers to introduce new lateral resistant steel moment frames such as seismic braced frames and hybrid steel frames. Hybrid steel frame is a new system which is based on introducing energy dissipating mechanism in the structural frame systems by replacing selected rigid connections with ductile energy dissipation semi-rigid connections [2]. Excessive inter-story drift was a major concern for using semi-rigid connections in steel frames [3]. This increase in the story drift in the hybrid frame at the floor levels with semi-rigid connections translates into connection rotation. This rotation forces the connections to behave in different manners depending on their geometric parameters such as bolt, angle /plate, beam and column size. For example, if the bolt diameter is small compared to the end-plate/angle thickness, the story drift translates to bolt elongation, which causes plate separation that ultimately leads to connection failure [3]. On the other hand, the desirable scenario is when the plate thickness is smaller than the bolt diameter in which the story drift translates into end-plate/angle yielding and causes fat hysteresis loops with or without pinching depending on the connection type [3]. The capability of the semi-rigid connections to withstand large plastic rotation (in excess of 0.05 radians) without failure was observed by several researches among with Astaneh et al. (1989) and Shen and Astaneh (2000) are noted here [4-5]. Properly design semi-rigid connections can undergo rotations without bolt or weld fracture up to 0.05 rad with fat hysteresis [4]. Thus, the increase story drift at the semi-rigid connection levels in hybrid frames doesn't necessarily have a negative impact. Indeed, if the connection rotation is observed by the plate or angle cyclic deformation (yielding), some of the yielded connections are replaceable after an earthquake event [3].

Many researchers studied the effects of semi-rigid connections within the SAC program but in those studies all the connections were considered as partially restrained. However the knowledge about the effect of semi-rigid connections in a hybrid frame is limited. In this study selected rigid connections are replaced by ductile semi-rigid connections in the 9-story SAC frame. Different patterns for locations of semi-rigid connections within the frames are examined and the results of normalized base shear, energy dissipation and maximum story drift angle are compared. Finally the frame with best performance is chosen.

## MODELING ASSUMPTION

### SAC frame Description

Design of SAC special steel moment resisting frames (SMRF) was performed as a part of the FEMA/SAC joint venture phase 2 studies on behavior of steel structures under seismic loading. These frames include a low-rise frame (3-story) , a mid-rise frame (9-story) , and a high-rise frame (20-story) which have been designed for three different locations that lie in seismic zones 2A (Boston),3 (Seattle) and 4 (Los Angeles) [1]. These buildings are designed as standard office building situated on soil type 2 (stiff soil) according to UBC 94. The 9-story SAC frame of the Los Angeles site are chosen for this study and modeled in OPENSEES. Floor plan and elevation of this frame are shown in Fig. (1). The details of sections and loadings are presented in FEMA355-C [1].

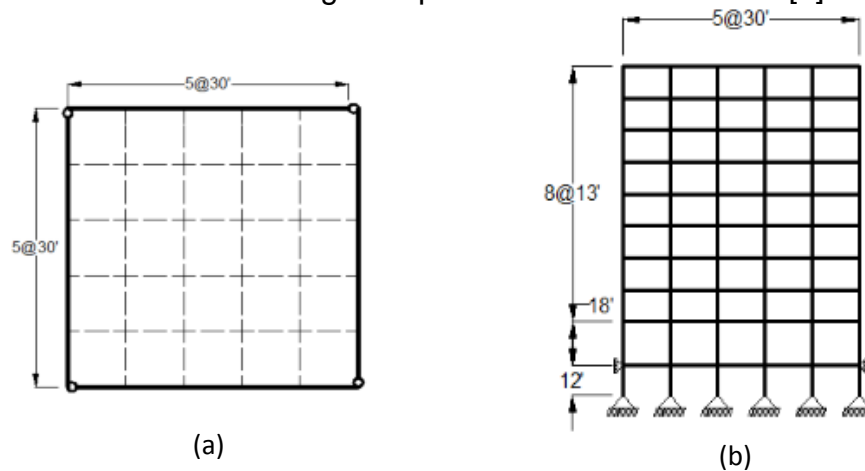


Fig. (1) Floor plan and elevation for 9-story SAC Los Angeles building [1].

a) Floor plan      b) elevation

### Modeling of ductile components

Plastic hinges in beams and semi-rigid connections are the main sources of nonlinearity. Beams with rigid connections as shown in Fig. (2) are modeled as compound elements which consists of an elastic Bernouli beam element at the middle confined by two plastic hinges and two end-zones that connects the member to the rigid connections. Non-linear behavior is introduced to the compound element explained above by introducing non-linear moment-rotation behavior of the plastic hinges. Other components of the compound including elastic beam elements and stiff end zones are assumed elastic.

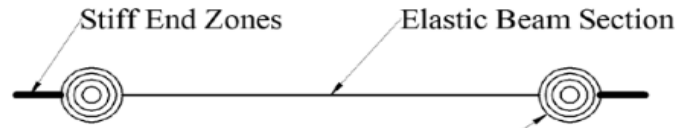


Fig. (2) Beam compound with stiff end zone and plastic hinges [6].

The semi-rigid beam compounds as shown in Fig. (3) are defined by replacing the two stiff end zones by two non-linear moment-rotation semi-rigid hinges in the rigid beam compounds. In this configuration, since the plastic moment of semi-rigid connections are usually much smaller than the plastic moment of beam sections, the behavior of the beam compound is governed by the behavior of the semi-rigid connections.

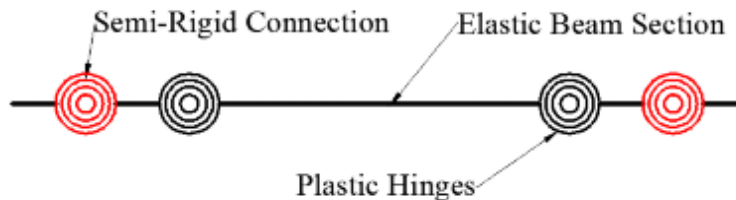


Fig. (3) Beam compound with semi-rigid connections and plastic hinges [6].

### Nonlinear modeling of plastic hinge

In this paper, Ibarra-Krawinkler model is utilized for modeling of plastic hinges [7]. The nonlinear behavior of plastic hinges is commonly expressed by presenting their moment-rotation backbone curve. The backbone curve is a reference force-deformation relationship that defines the bounds within which the hysteretic response of the component is confined [8]. A typical initial (monotonic) backbone curve and necessary definitions are illustrated in Fig. (4). The quantities  $F$  and  $\delta$  are generic force and deformation quantities. For flexural plastic hinge regions  $F = M$  (moment) and  $\delta = \theta$  (rotation). Refinements, such as more accurate multi-linear descriptions can be implemented as seemed necessary. The properties of the initial (monotonic) backbone curve in the positive and negative direction can be different, as necessitated, for instance, by the presence of a slab on a steel beam. Residual strength  $F_r$  is present in most steel components unless fracture occurs before the component strength stabilizes at a residual value [8]. The ultimate deformation capacity usually is associated with a sudden, catastrophic failure mode. In steel components, this can be ductile tearing associated with severe local buckling, or fracture

at weldments. It is possible that the ultimate deformation capacity  $\delta_u$  is smaller than the deformation at which a residual strength is reached  $\delta_r$  [8].

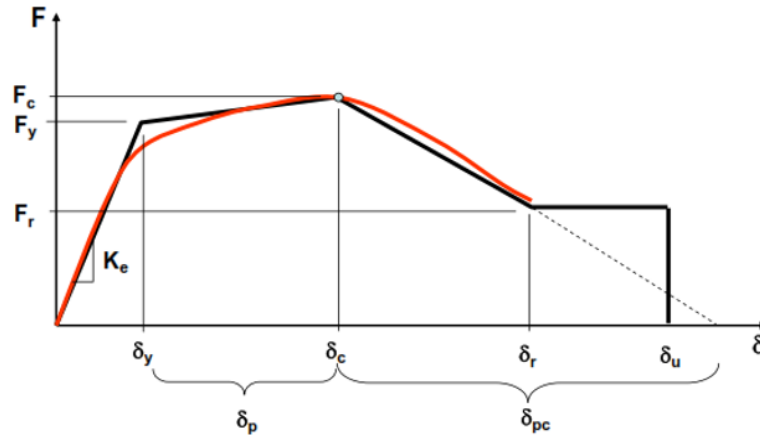


Fig. (4) Parameters of the initial (monotonic) backbone curve of the Ibarra-Krawinkler model [8].

Ibarra-krawinkler empirical equations based on multi-variate regression analysis that account for combination of geometric and material parameters in the quantification of modeling parameters are used here. The experimental results documented in Lignos and Krawinkler (2007, 2009) are also utilized to some extent in FEMA 355D and ASCE/41-06 seismic Rehabilitation of existing building [9-10]. The following equations are suggested to estimate modeling parameters as a function of geometric and material parameters that were found to be statically significant [8].

$$\theta_p = 0.087 \cdot \left(\frac{h}{t_w}\right)^{-0.365} \cdot \left(\frac{b_f}{2 \cdot t_f}\right)^{-0.14} \cdot \left(\frac{L}{d}\right)^{0.34} \cdot \left(\frac{d}{c_{unit}^{1.21''}}\right)^{-0.721} \cdot \left(\frac{c_{unit}^2 \cdot F_y}{50}\right)^{-0.23} \quad (1)$$

$$\theta_{pc} = 5.70 \cdot \left(\frac{h}{t_w}\right)^{-0.565} \cdot \left(\frac{b_f}{2 \cdot t_f}\right)^{-0.8} \cdot \left(\frac{d}{c_{unit}^{1.21''}}\right)^{-0.28} \cdot \left(\frac{c_{unit}^2 \cdot F_y}{50}\right)^{-0.43} \quad (2)$$

Where the parameters used in these equations are defined as:

$h/t_w$  = ratio of fillet-to-fillet depth to web thickness.

$b_f / 2t_f$  = ratio of flange width to thickness.

$L/d$  = ratio of shear span to depth.

$d$  =depth of beam.

$F_y$  = yield strength of the flange in ksi.

$c_{unit}^1$  = (and  $c_{unit}^2$ ) coefficients for units conversion. If  $d$  is in meters and  $F_y$  is in MPa  
 $c_{unit}^1 = 0.0254$  and  $c_{unit}^2 = 0.145$ . Both coefficient are 1.0 if inches and ksi are used.

Lignos and Krawinkler (2009) report a mean value for  $M_y$  of  $1.17M_p$ , with  $M_p = Z \cdot F_y$  where  $F_y$  is the measured flange yield stress [10]. A value of  $M_y = 1.1 M_p$  is recommended with  $M_p$  based on the expected yield stress [8]. Also Lignos and Krawinkler report a mean value of the ratio of capping strength to effective yield strength  $M_c/M_y$  of 1.11 [10]. A value of 1.1 for this ratio is recommended in both cases [8]. Data in Lignos and Krawinkler suggest that a reasonable estimate of residual strength would be 0.4 times the effective yield strength,  $M_y$  [10].

## Modeling of semi-rigid connection

Hybrid frames have semi-rigid beam to column connections. A typical sketch of the top and seat-angle with double web angle connections selected as a semi-rigid connection for this study, is shown in Fig. (5). This connection is modeled for six different beam sections of W21X50, W24X62, W27X84, W30X99, W33X141 and W36X150 that covers all the beam depths used in SAC frames by Razavi et.al [6]. A 3-D finite element model of the top-and seat-angle with double web angle connections is presented in Fig. (6). The semi-rigid connection properties presented in Table. (1), were calculated by Razavi et.al and used in this study [6]. In this table  $\theta_y$  and  $M_y$  are yield rotation and yield moment,  $\theta_u$  and  $M_u$  are ultimate rotation and moment,  $k_0$  and  $k_1$  are elastic and plastic stiffness respectively.

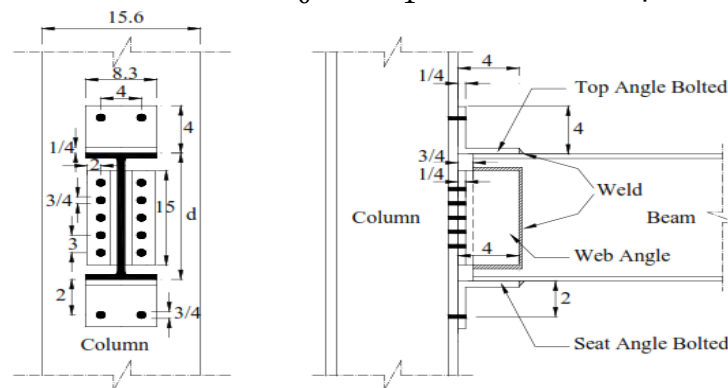


Fig. (5) Typical sketch of top-and seat-angle with double web angle connections [6].

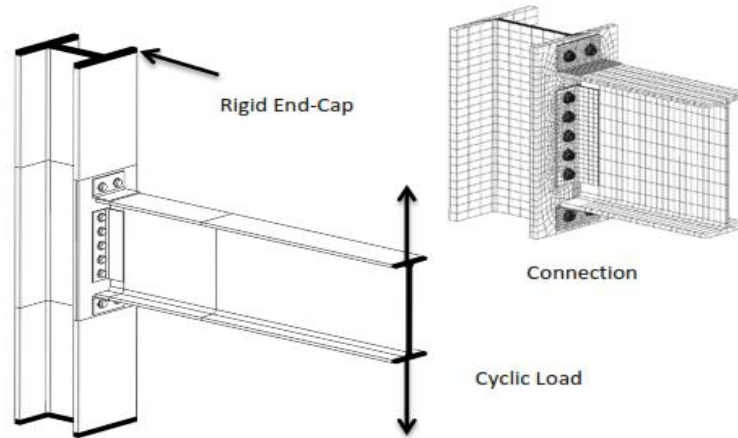


Fig. (6) Top and seat- angle with double web angle finite element model, and mesh properties [6].

Table. (1) Semi-rigid connections properties [6].

Beam size		(kip-in)		(kip-in)		
W21x50	0.003	1032	0.05	1750	344000	15277
W24x62	0.003	1203	0.05	2000	401000	16957
W27x84	0.003	1411	0.05	2250	470333	17851
W30x99	0.003	1584	0.05	2450	528000	18426
W33x141	0.003	1920	0.05	2900	640000	20851
W36x150	0.003	2080	0.05	3300	693333	25957

### Hybrid frame pattern selection

In this section ,13 hybrid frames with several different patterns of semi-rigid connection replacements within the frame are selected Fig. (7) - Fig. (10) .In addition to hybrid frames an original SAC frame with rigid beam to column connections is considered . Hybrid frames are designated az HSAC9 and marked from 1 to 13 as shown in Fig. (7) - Fig. (10). They are categorized in three main groups based on the number of semi-rigid connections. Group1, HSAC9-1 to HSAC9-3 have 18 semi-rigid connections. Group2, HSAC9-4 to HSAC9-10 have 30 semi-rigid connections. Group3, HSAC9-11 to HSAC9-13 have 36 semi-rigid connections. All the frames are subjected to static pushover analysis, cyclic displacement history and nonlinear dynamic analysis. The results are discussed in the next sections and finally the frame with best performance is chosen.

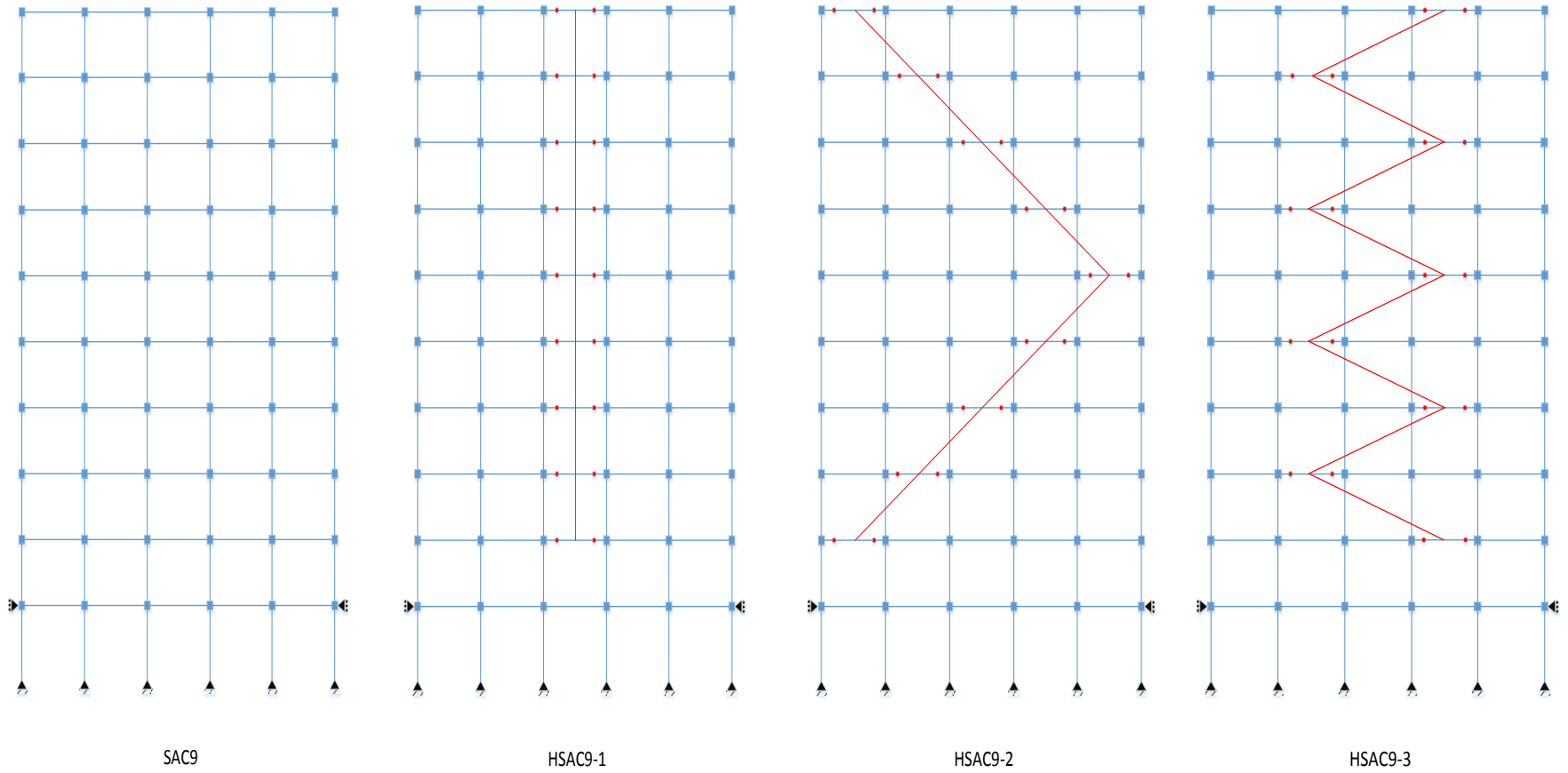


Fig. (7) Original SAC frame and Hybrid models for 9-story frames

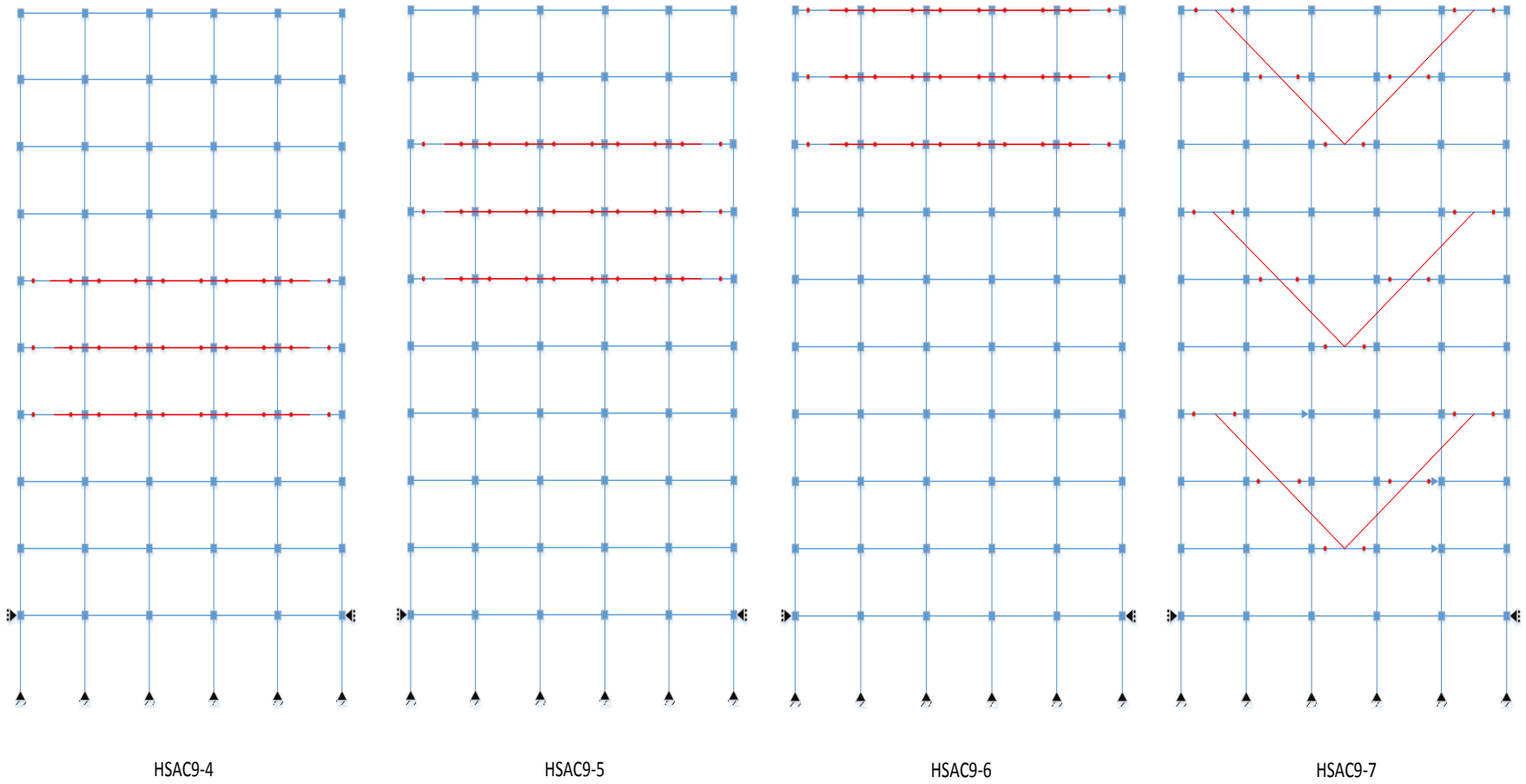


Fig. (8) Hybrid models for 9-story frames

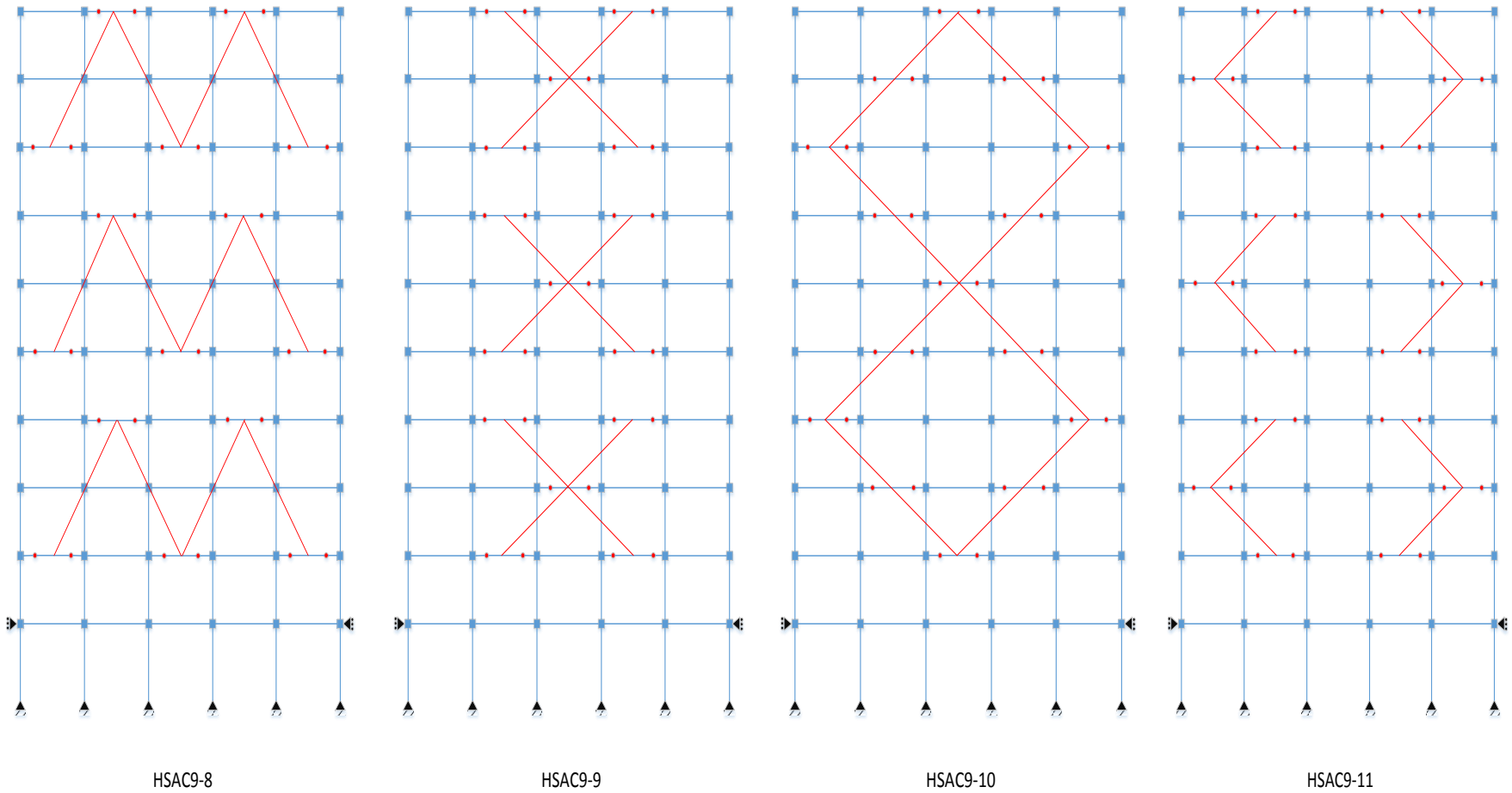
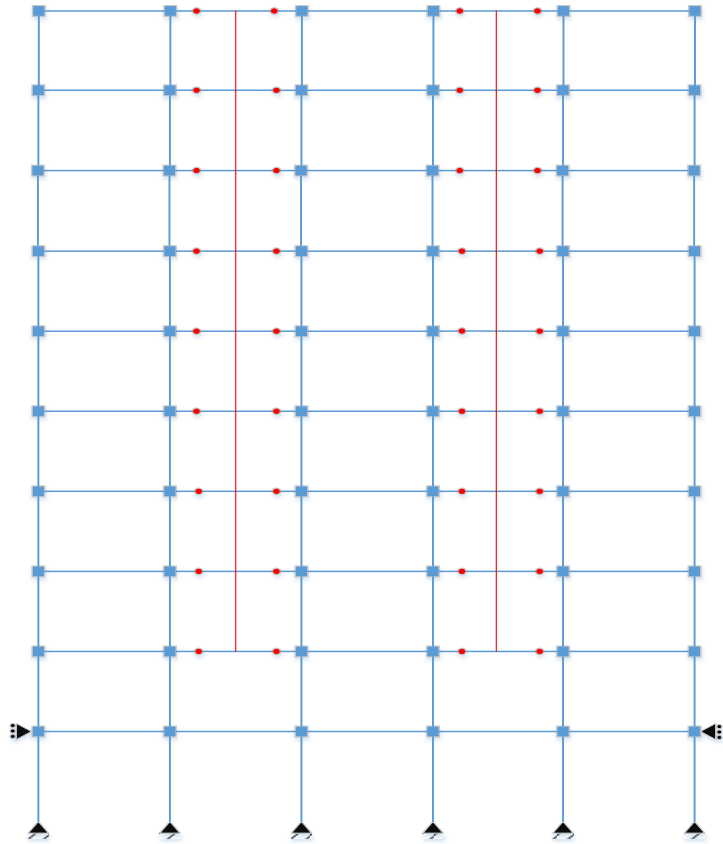
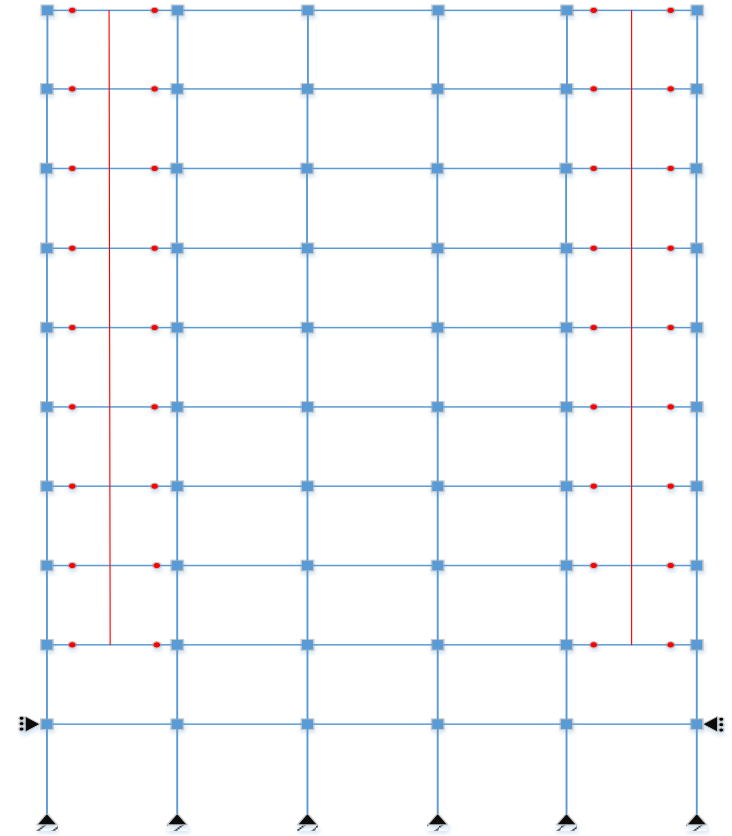


Fig. (9) Hybrid models for 9-story frames



HSAC9-12



HSAC9-13

Fig. (10) Hybrid models for 9-story frames

## Results and discussions

### Static pushover analysis

The selected frames are subjected to nonlinear static pushover analysis also up to roof drift of 6 percent. All the resultant pushover curves for hybrid frames and SAC frame are plotted in Fig. (11). As explained in previous sections, hybrid frames are obtained by replacing a selection of fully rigid connections with more flexible semi-rigid connections consequently a more flexible stiffness matrix for hybrid frames is expected. As shown in Fig. (11) both initial stiffness and base shear are decreased in the hybrid frames. However since using semi-rigid connection will reduce the system's stiffness, the optimum number and pattern of semi-rigid connections should be determined to find the minimum base shear which still satisfies the inter-story drift limits. The maximum normalized base shear for all the frames are sorted in table. (2). As shown in table. (2), SAC9 and HSAC9-4 have the maximum and minimum base shear demands respectively. Other frames have the base shear demands between the two extremes.

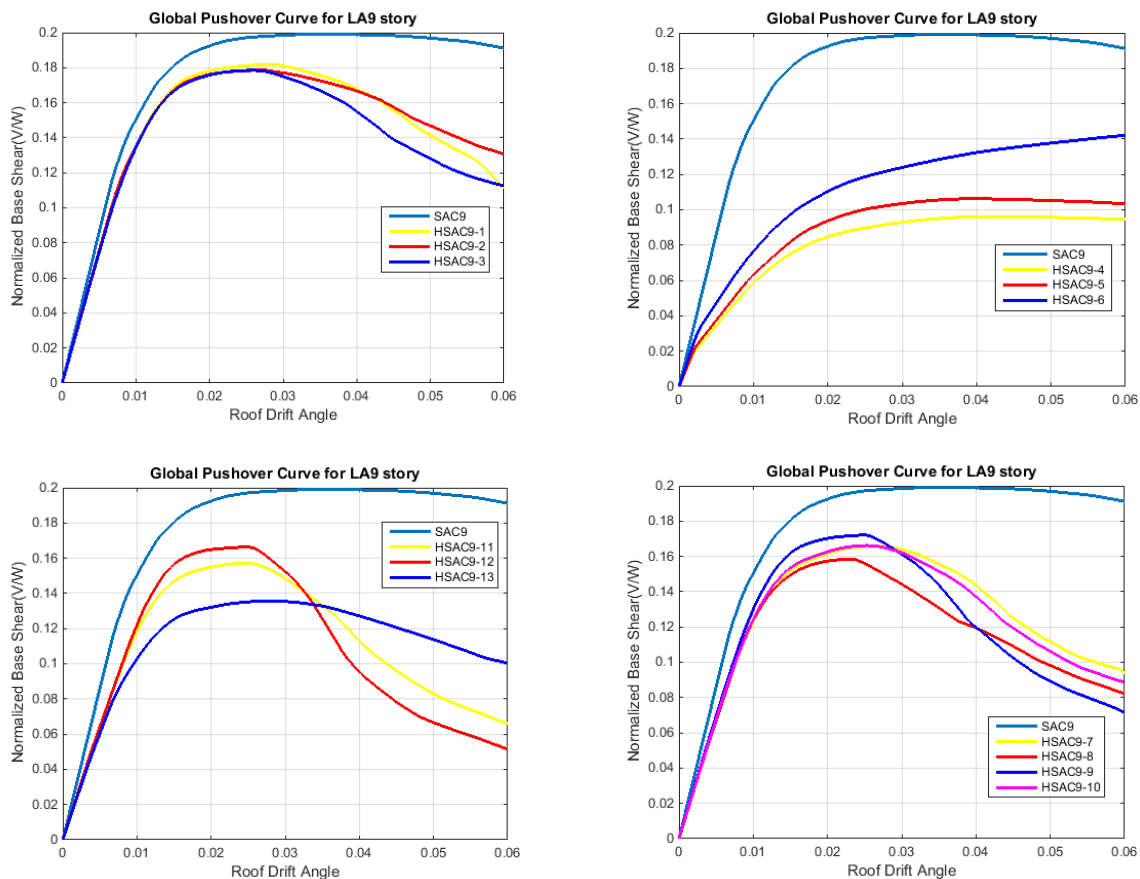


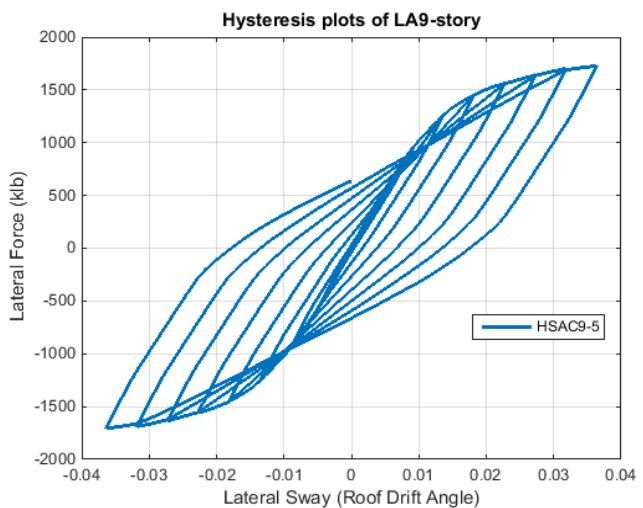
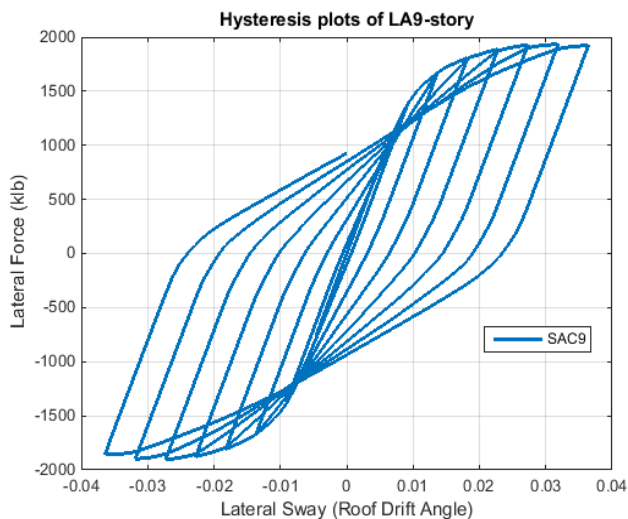
Fig. (11) Global Pushover Curves for LA 9-story Structures

Table. (2) Maximum base shear demands in the selected frames (V/W)

HSAC 9-4	HSAC 9-5	HSAC 9-13	HSAC 9-6	HSAC 9-11	HSAC 9-8	HSAC 9-7	HSAC 9-10	HSAC 9-12	HSAC 9-9	HSAC 9-3	HSAC 9-2	HSAC 9-1	SA C9
0.091	0.106	0.136	0.143	0.157	0.158	0.165	0.166	0.167	0.172	0.178	0.179	0.182	0.2

### Cyclic displacement history analysis

In the next step, all the frames are subjected to a cyclic displacement history designed to be capable of producing 0.035 lateral sway (Roof drift angle) in order to ensure yielding and subsequent inelastic hysteresis behavior in all the semi-rigid connections. The energy dissipation of each frame is examined by plotting the building's lateral force-sway hysteresis loops as shown in Fig. (12). The area under the outer loop is calculated for each hysteresis plot of Fig. (12) which indicates the effectiveness of the semi-rigid pattern and frame's energy dissipation capability as shown in table. (3). It should be noted that the plastic moment of semi-rigid connections is generally less than the plastic moment in their adjacent frame beams thus, the moment cannot exceed the plastic moment of the connection and formation of plastic hinges in the adjacent beams will be avoided. Since the amount of energy dissipated by semi-rigid connection is less than plastic hinge, the hybrid frames have less amount of dissipated energy. As shown in table. (3), SAC9 and HSAC9-5 have the maximum and minimum energy dissipation amount, other frames are



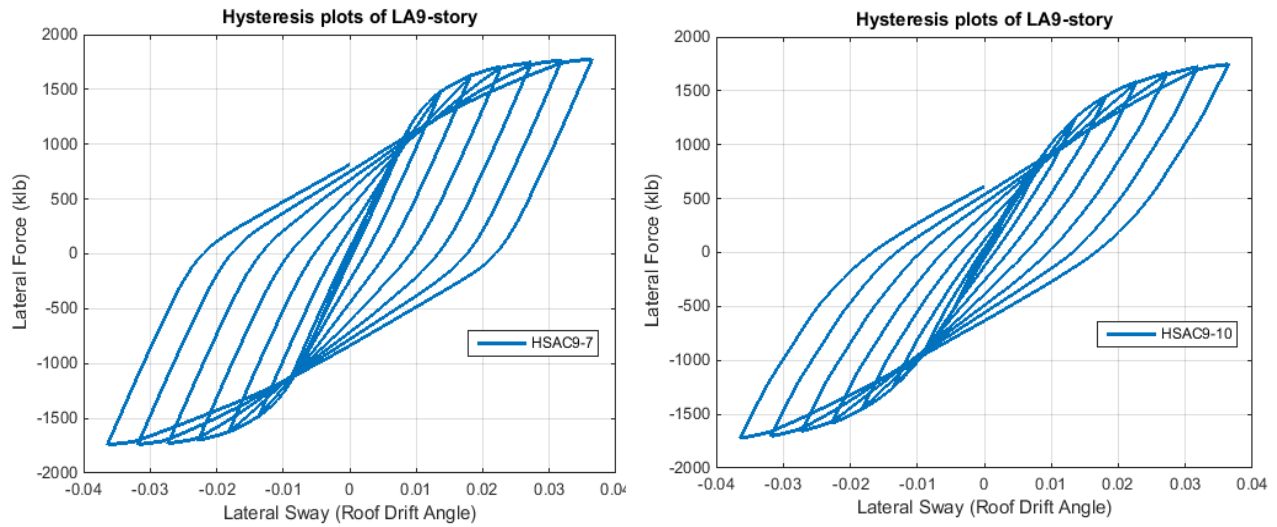


Fig. (12) lateral force –sway hysteresis loops of the selected frames

Table. (3) Energy dissipation of the selected frames (klb)

HSAC 9-5	HSAC 9-4	HSAC 9-6	HSAC 9-13	HSAC 9-11	HSAC 9-9	HSAC 9-12	HSAC 9-10	HSAC 9-7	HSAC 9-8	HSAC 9-1	HSAC 9-3	HSAC 9-2	SA C9
189.3	194	198	230.4	262.5	268.7	270.1	272.7	273.2	276.5	298.6	298.8	299.6	331

### Nonlinear dynamic analysis

A major concern about using semi-rigid connection in steel frames is that it may cause the inter-story drifts to increase beyond acceptable limits [11]. Although the use of hybrid frame causes decrease in the initial stiffness, however, ground motions do not act similar to static lateral loads on the frame. Ground motions exert forces to frames by introducing acceleration to stories' mass in story levels. Since semi-rigid connections shift the period of structures, the amount of acceleration will not remain constant. On the other hand, although the initial stiffness of a SMRF is more than the initial stiffness of its corresponding hybrid frame, the system stiffness of the frame changes during an earthquake due to yielding in structural members and nonlinear moment-rotation behavior of semi-rigid connections [6].

All the frames are subjected to the SAC ground motions for the Los Angeles site. These ground motions are categorized in two levels of Design Based Earthquake (DBE) and

Maximum Credible Earthquake (MCE) based on their return period. The models are first subjected to the set of 20 DBE records, LA01 to LA21, to be evaluated for the first performance objective which is to satisfy the Life Safety (LS) performance under DBE hazard level Fig. (13). The passing criterion for this performance objective is to maintain an average inter-story drift of less than 2.5%. The results show that only SAC9 , HSAC9-1 HSAC9-2 and HSAC9-8 satisfy the LS criterion table. (4).

The frames are then subjected to the set of 20 MCE records, LA21 to LA40 , to be evaluated for the second performance objective , which is to satisfy the Collapse Prevention (CP) performance under the MCE hazard level Fig. (14). The passing criterion for this performance objective is to maintain an average inter-story drift of less than 5%. The results show that All the frames pass CP criterion except HSAC9-4 , HSAC9-5 and HSAC9-6 table. (5).

Table. (4) Maximum Story Drift Angle for selected frames subjected to L.A.DBE records

HSAC9-2	HSAC9-8	SAC9	HSAC9-1
0.024221	0.02441	0.02443	0.02494

Table. (5) Maximum Story Drift Angle for selected frames subjected to L.A.MCE records

HSAC9-4	HSAC9-6	HSAC9-5
0.05076	0.06208	0.06214

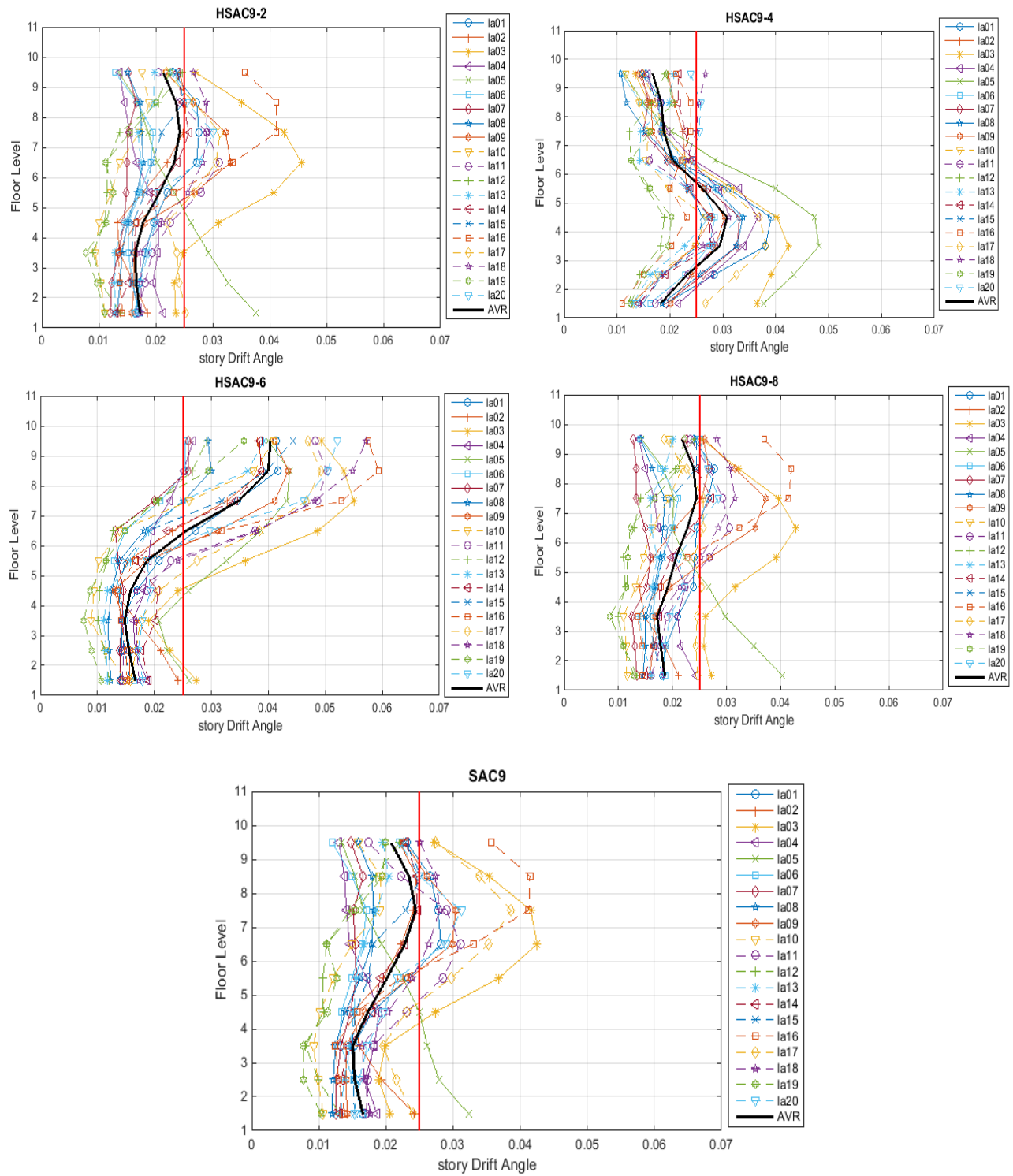


Fig. (13) Story Drift diagrams for selected frames subjected to L.A.DBE records

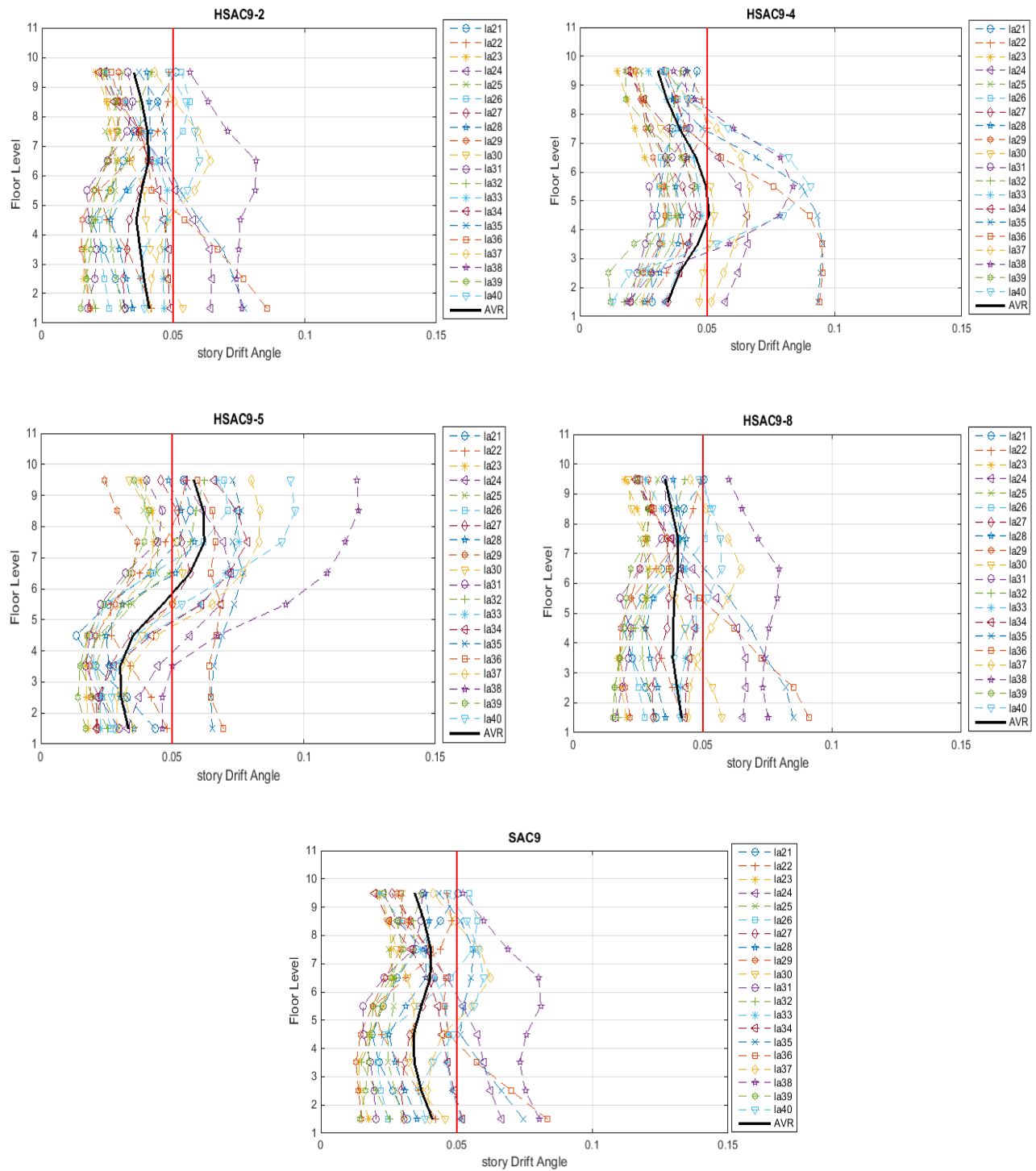


Fig. (14) Story Drift diagrams for selected frames subjected to L.A.MCE records

## **CONCLUSION**

In this paper, several different patterns and locations of semi-rigid connection replacements within the frame are examined for the 9-story SAC frame in order to identify the hybrid frame with the best seismic performance. All the frames are subjected to static pushover analysis, cyclic displacement history and nonlinear dynamic analysis. The frames are compared based on their maximum normalized base shear, energy dissipation and maximum story drift angle during L.A records. The results show all the hybrid frames have the maximum base shear less than SAC frame, which is preferable and indicate the decrease in force demands in frame members. On the other hand, the amount of energy dissipated in hybrid frames are less than SAC frame, thus SAC frame has more energy dissipation capacity. On average, inter story drift angle in hybrid frames are more than SAC frame. This increase are acceptable until it satisfies LS criterion. Only 4 frames of SAC9 HSAC9-1, HSAC9-2 and HSAC9-8 pass the 2.5% limit. the results of MCE records show that all the frames pass the CP criterion except HSAC9-4, HSAC9-5 HSAC9-6. Considering all the results and the tendency of engineers to design a frame with less base shear, more energy dissipation capacity and less inter story drift angle, the HSAC9-8 is desirable option. It passes the LS and CP criterion and its maximum base shear and energy dissipation are less and more than mean value respectively. Probably the key feature of this frame is uniform distribution of semi-rigid connections in the whole structure (both bays and stories). Concentration of semi-rigid connections in a specific region may cause the inter story-drifts to increase beyond acceptable limits.

## **REFERENCES**

- [1] FEMA, 2000b, State of the Art Report on System Performance of Steel Moment Frames Subject to Earthquake Ground Shaking, FEMA 355C Report, prepared by the SAC Joint Venture Partnership for the Federal Emergency Management Agency, Washington, D.C.
- [2] Abolmaali A, Razavi M, Radulova D. On the concept of earthquake resistant hybrid steel frames. *J Constr Steel Res* 2012; 68:34–42.
- [3] Abolmaali A, Kukreti AR, Motahari A, Ghassemieh M. Energy dissipation characteristics of semi-rigid connection. *J Constr Steel Res* 2009; 65:19–27.
- [4] Astaneh A, Nader MN, Malik L. Cyclic behavior of double angle connections. *J Struct Eng ASCE*1989 ; 115(5):1101–18.

- [5] Shen, J., and Astaneh-Asl, A. (2000), Hysteresis model of bolted-angle connections. *Journal of Construction Steel Research* 54, 317-343.
- [6] Abolmaali A, Razavi M, Radulova D., [2014], "Earthquake resistance frames with combination of rigid and semi-rigid connections". *Journal of Constructional Steel Research* 98pp. 1–11
- [7] Ibarra L.F., Medina R.A., and Krawinkler, H., [2005], "Hysteretic models that incorporate strength and stiffness deterioration," *Earthquake Engineering and Structural Dynamics*, Vol. 34, No. 12, pp. 1489-1511.
- [8] PEER, [2010], *Seismic Design Guidelines for Tall Buildings*, PEER Report 2010/05, Pacific Earthquake Engineering Research Center, University of California, Berkeley, California.
- [9] Lignos, D.G., and Krawinkler, H., [2007], "A database in support of modeling of component deterioration for collapse prediction of steel frame structures," *ASCE Structures Congress 2007*, Long Beach, California
- [10] Lignos, D. G., and Krawinkler, H. (2009). "Sidesway Collapse of Deteriorating Structural Systems under Seismic Excitations," Technical Report 172, The John A. Blume Earthquake Engineering Research Center, Department of Civil Engineering, Stanford University, Stanford, CA.
- [11] Gupta A, and Krawinkler, H., [1999], "Seismic Demands for performance evaluation of steel moment resisting frame structures". Department of Civil and Environmental Engineering Stanford University, Report No. 132. June 1999.